Epoxy Adhesives with Reversible Hardeners: Controllable Thermal Debonding in Bulk and at Interfaces

Filip Van Lijsebetten, Tim Maiheu, Johan M. Winne and Filip E. Du Prez**

Polymer Chemistry Research group, Centre of Macromolecular Chemistry (CMaC) and Laboratory of Organic Synthesis, Department of Organic and Macromolecular Chemistry, Faculty of Sciences, Ghent University, Krijgslaan 281-S4, Ghent, 9000, Belgium.

E-mail: Filip.DuPrez@UGent.be; Johan.Winne@UGent.be

KEYWORDS. Covalent adaptable networks, neighbouring group participation, recyclable thermoset, debondable adhesives

ABSTRACT

On-demand adhesive dismantling has the potential to improve multi-material product recycling, but its implementation has been hampered by a critical trade-off between strong bonding and easy debonding. As a result, the temperature range in which these temporary adhesives can be used is relatively limited. Here, we report a new class of dynamic epoxy resins that significantly extends this upper temperature limit and still achieves fast debonding. Specifically, two types of dynamic polyamidoamine curing agents for epoxy hardening were developed, being polysuccinamides (PSA) and polyglutaramides (PGA). As the dynamic debonding/rebonding process of PSA and especially PGA linkages is more thermally demanding and at the same time more thermally robust than previously reported dynamic covalent systems, the resulting materials can be triggered at high temperatures, and at the same time remain bonded over a wide temperature range. The versatility of the PSA and PGA dynamic adhesive curing system was demonstrated in classical bulk adhesive formulations, as well as in dynamic covalent linking to a PSA- or PGA-functionalised surface. As a result, an attractive drop-in strategy was achieved for producing debondable and rebondable epoxy adhesives, with high complementarity to existing adhesive resin technologies and applicable in an industrially relevant temperature window.

INTRODUCTION

The ability to separate multi-layered structures without damaging the bonded substrates is quite appealing for applications in electronics, dentistry and construction.[1–3] While many debonding technologies exist, such as thermally expandable particles (Apple Inc. technology) and solvent-based detachment (US Air Force),[1,4,5] developing approaches that are functional, industrially relevant, and allow removal only upon activation is particularly difficult. Furthermore, not all adhesives work in the same way. Pressure sensitive adhesives, for example, must be approximately 13 000 times weaker than structural adhesives in order to function.[6] Nonetheless, these design challenges can be addressed by using heat-triggerable "temporary adhesives" that start from existing polymer matrices and provide reliable changes in physical properties to separate bonded substrates.[7]

Temporary adhesives are unique in that interactions at the interface (*i.e.* adhesion) and within the bulk (*i.e.* cohesion) can be controlled or programmed independently. Critically, the precise mechanism that will promote debonding will be dependent on the molecular design of the adhesive. While early reports in this field focused on supramolecular adhesives,[8,9] dynamic covalent systems provide an intriguing alternative when stronger bonding is required during use.[7,10–13] Several examples of recent chemical platforms used for temperature-induced debonding include disulfide exchange,[14–17] Diels-Alder chemistry,[18–23] transesterification,[24] and boronic ester transesterification.[25–27] Especially the well-reported furan-maleimide Diels-Alder system has attracted both academic and industrial attention with respect to its temporary properties (**Figure 1a, top**).[28–33]

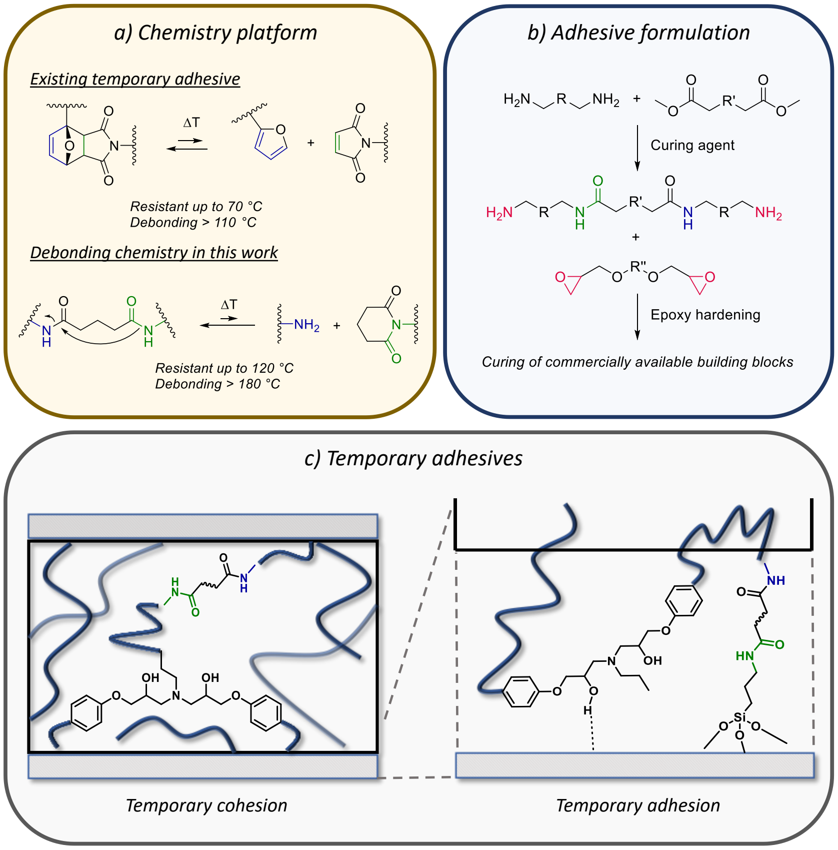

Figure 1. Schematic overview of the applied research strategy to design novel robust and reversible epoxy adhesives. a) Existing furan-maleimide reversible adhesives (top) and the previously reported dicarboxamide debonding equilibrium to a cyclic imide and amine used in this work (bottom).[34] b) Easy implementation of dynamic polysuccinamide (PSA) and polyglutaramide (PGA) curing agents into epoxy formulations. c) Temporary adhesion could be achieved through variation in both the level of cohesion and adhesion as a function of temperature.

However, widespread adoption of the furan-maleimide system has been limited due to significant debonding at temperatures below 100 °C and frequent complete liquification around 120 °C.[23,35,36] Furthermore, the (re)generated furan and maleimide groups are not thermally robust and can undergo a variety of side reactions upon heating, including homopolymerisation of the maleimides.[34] Therefore, it is of great interest to investigate other chemical platforms that enable a more reliable and controlled introduction of dynamic covalent behaviour into larger volume bulk materials without the risk of unintended debonding.[37] In this context, thermally more demanding systems are a better choice for investigating the effect of debonding in matrices where strong bonding is desired, such as for (semi-)structural adhesives.

Structural adhesives are key to building lightweight structures for objects used in major industries such as energy, construction, and the automotive sector.[38–40] Typical formulations include a flowable mixture that reacts and cross-links into polyacrylate, polyurethane or epoxy resins.[41–43] Epoxy thermosets are arguably one of the most relevant structural adhesive classes, where (dynamic) properties can be introduced through a variety of curing agents, resins, modifiers, and fillers.[44–52] More specifically, polyamide hardeners for epoxy systems are a well-known functional type of amino polyamide curing agents and they are frequently used to add flexibility and toughness to traditional epoxy formulations without sacrificing thermal stability.[46,53–56] Nonetheless, because of their inherent bond strength, amide bonds are generally thought to be irreversible due do their molecular design.

More recently, our research group, as well as the groups of Sijbesma, Heuts and co-workers, found that polyamide backbones can in fact be designed to undergo a reversible thermal debonding without the need for catalysts or additives, *via* cyclic imide formation (**Figure 1a, bottom**).[57,58] In comparison to the well-known furan-maleimide system and other intrinsically weaker cross-linkages, debonding occurs only at significantly higher (and tuneable) temperatures by shifting the equilibrium between dicarboxamides and cyclic imides. Consequently, this was the starting point to explore the potential of this reversible polyamide platform in epoxy resin adhesive formulations and applications.

Herein, we report the outcome of our studies, with a particular focus on polysuccinamide (PSA) and polyglutaramide (PGA) as dynamic epoxy hardeners, which have shown attractive reactivity profiles for the design of debondable adhesives. PSA and PGA hardeners can be easily prepared from a variety of classical diamine hardeners by simple treatment with either dimethyl succinate or dimethyl glutarate (**Figure 1b**). Their ready implementation into epoxy adhesive technologies was demonstrated in debonding in the bulk of adhesives, as well as at the interface with functionalized surfaces (**Figure 1c**). To accomplish this, cyclic imide-based silane primers (as PSA or PGA precursors) were developed and coated onto a surface before reversible amide linkages could form across the adhesive-adherend interface during epoxy curing. The choice between PSA and PGA linkages allows tuning of the dynamic properties, even independently at the surface and in the bulk, by using different linkage chemistries at both sites. As such, it could be tested if both cohesive and adhesive forces could be tuned as a function of temperature to afford reliable temporary adhesion. A thorough examination of tensile properties, stress-relaxation, frequency sweep, and creep experiments enabled the most desirable mechanical and viscoelastic properties to be determined. X-ray photoelectron spectroscopy (XPS) and atomic force microscopy (AFM) were used to determine the deposition of the silane primer, and differences in adhesion strength were investigated using lap-shear experiments.

RESULTS AND DISCUSSION

Synthesis of dynamic curing agents

As a first research objective, we investigated the design of possible dynamic amino polyamide curing agents. Polyamide and amidoamine curing agents, such as Ancamide® (Evonik industries), are widely used in a variety of markets, including adhesives, coatings, composites, and electrical encapsulation.[46] Usually, they are synthesised by reacting C_{36} dimer fatty acids with an excess of polyethylene polyamines, resulting in low to highly viscous hardeners.[59] As a result, as opposed to the well-known semi-crystalline nylon, amorphous prepolymers are obtained with a significant amount of amine terminating groups. However, these traditional cross-linkers do not afford reprocessable or thermally debondable epoxy materials.

Because polysuccinamides and polyglutaramides are easy to synthesise, a wide range of polyamide hardener formulations can be investigated. As a result, many options are directly accessible by substituting the dimer fatty acid in classical polyamide formulations for the dimethyl esters of either succinic acid or glutaric acid, or both. The three formulations that were further investigated in this work were chosen to show the versatility of the system and were also found to offer a good balance between adhesion, flexibility and mechanical strength. To start, an amine mixture was prepared by mixing 0.36 eq. Priamine 1074 (**1**), 0.36 eq. 2,2,4(2,4,4)-trimethyl-1,6-hexanediamine (**2**), 0.12 eq. triethylenetetramine (**3**) and 0.36 eq. 1,3-cyclohexanebis(methylamine) (**4**, **Figure 2**). Each amine building block was specifically chosen to offer a good balance of adhesion, flexibility, and mechanical strength. Important for eventual epoxy curing, this corresponded to a total of 5.04 eq. NH functionalities when all primary and secondary amines of each monomer were considered.

The aforementioned mixture could then be used for either immediate conventional amine hardening of epoxies (irreversible) or to initiate a polycondensation reaction with almost any dibasic ester monomer, yielding a dynamic polyamide hardener for subsequent epoxy curing (reversible). First, a non-debondable epoxy reference (ER) was created upon immediate reaction with bisphenol A diglycidyl ether (BADGE, **8**) in a molar epoxy-to-amine ratio (E/NH) of 1.0 (**Figure 2a**). This benchmark material could be used to compare the viscoelastic and thermomechanical properties of the dynamic epoxy resins (*vide infra*).

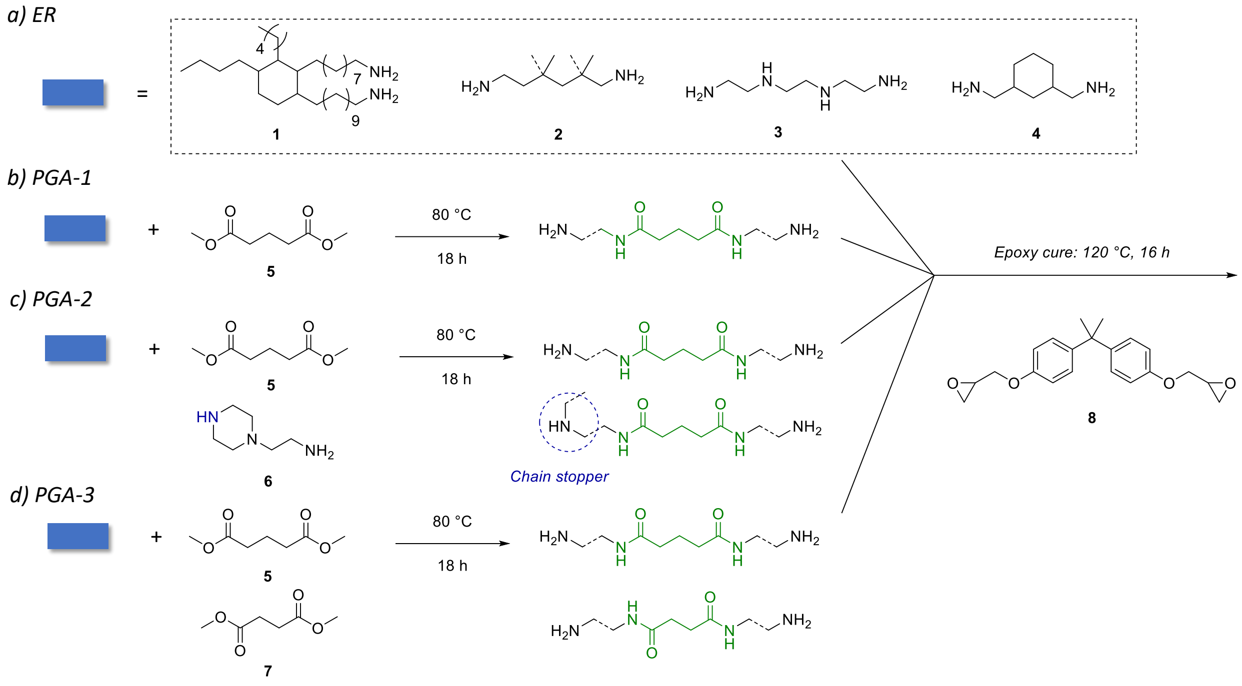

Figure 2. Schematic overview of epoxy curing procedure. a) an epoxy reference (ER) was prepared by reacting an amine mixture with bisphenol A diglycidyl ether. For the dynamic epoxy materials, prior to material curing, a polyamide curing agent was prepared for b) PGA-1, c) PGA-2 and d) PGA-4 by polycondensation of the corresponding ester(s).

In a second step, the general amine mixture was used for a polycondensation reaction with dimethyl glutarate (**5**) in a molar ester-to-amine ratio (ESTER/NH_2) of 0.83 at 80 °C for 16 h, yielding a robust PGA curing agent (PGA-1, **Figure 2b**). Since it was desirable to obtain a polyamide with two amine end groups, a stoichiometric excess of 1.04 eq. NH groups was theoretically calculated, which was incapable of further chain-growth when all the dibasic ester monomer was consumed. As a result, roughly 65 mol% of the available NH groups was reacted to a dynamic amide bond, which was necessary to endow sufficient reversible behaviour. Indeed, as evidenced by Torkelson and co-workers,[60] further increasing the excess of NH functionalities can lead to a relatively larger amount of static or permanent bonds, hampering material flow.

A way to tune the degree of polymerisation, without the need to increase the excess of NH functionalities and reduce the amount of dynamic amide bonds, was to substitute a portion (0.06 eq.) of amine compound (**2**) in the amine mixture for 2-(1-piperazinyl)ethylamine (**6**, PGA-2, **Figure 2c**). The use of such a reactive diluent is commonly known for epoxy curing,[54] further highlighting the drop-in nature of the reported strategy. The secondary amine of compound **6** was expected to be more sterically hindered to react with dimethyl glutarate than the more accessible primary amines and could thus act as a chain stopper. As a result, addition of **6** increased the relative amount of secondary amine chain-ends while decreasing the total amount of excess "NH" groups to 0.98 eq. and keeping roughly 67 mol% dynamic amide bonds.

The development of a PSA curing agent for adhesive applications was more difficult because they were found to be too dynamic, as preliminary studies and different formulations showed significant debonding at lower T (**Figure S1-S2**). However, given the intended application, reversible behaviour can be induced in a lower user-defined temperature window by simply replacing a portion (40%) of the dimethyl glutarate with the more reactive succinate ester (**7**) mixture (PGA-3, **Figure 2d**). Finally, after using each prior mentioned hardener to cure the epoxy compound **8** at 120 °C for 5 h under vacuum, ATR-FTIR analysis and Soxhlet extraction with THF were used to verify network formation (see **Table 1** and **Figure S3-S4**).

Table 1. Overview of thermomechanical properties and relaxation data of the (modified) epoxy networks

Epoxy network	T_g[a] (°C)	$T_{d5\%}$[b] (°C)	Swel. Rat.[c] (%)	Sol. Frac.[d] (%)	$\tau^*_{250\ °C}$[e] (s)	$\tau^*_{200\ °C}$[e] (s)	E[f] (MPa)	W[f] (MJ.m^{-3})
PGA-1	46	353	140 ± 3	2 ± 0.5	390	183 095	345 ± 80	1350 ± 326
PGA-2	54	353	123 ± 2	1 ± 0.2	430	105 310	765 ± 110	4035 ± 303
PGA-3	43	352	124 ± 16	7 ± 0.7	785	189 055	330 ± 66	760 ± 57
ER	62	347	106 ± 2	1 ± 0.3	-	-	845 ± 160	398 ± 84

[a] Determined from the second heating in DSC analysis (10 °C.min^{-1}). [b] TGA onset temperatures after 5% weight loss ($T_{d5\%}$). [c] Swelling ratio obtained from a four-sample measurement in THF at rt for 24 h. [d] Soluble fraction was obtained from Soxhlet extraction in THF for 24 h. [e] Calculated relaxation time (τ^*) obtained by fitting to a stretched single exponential decay. [f] Apparent Young's modulus (E) and toughness (W) determined from tensile testing performed at 20 °C (preload 0.05 N and 10 mm.min^{-1}). These values are relative and for comparison purposes only.

Thermal and mechanical properties

To ensure the dynamic cross-linker would not have a negative impact on thermal stability, DSC and TGA analysis were performed to determine thermal properties. Promising results could be obtained with glass transition temperature (T_g) values in the range of 43 to 62 °C and $T_{d5\%}$ values situated around 355 °C (**Figure S5-S6**). Furthermore, due to the thermally demanding dynamic behaviour (*i.e.* cyclisation to a glutarimide) and higher cross-linking density (*i.e.* more restricted chain diffusion) of PGA-1 to PGA-3, it was hypothesised that (re)processing would necessitate additional heating.[57] However, it was critical to ensure that such thermoplastic processing temperatures did not result in excessive oxidation or degradation of the polymer material. Isothermal TGA experiments at 250 °C for 2 h revealed only 1.5% weight loss (**Figure S7**). Surprisingly, when compared to our previously reported dynamic polyamide materials in a non-epoxy based matrix (PA ref, **Figure 3a**),[57] the herein reported PGA-cured materials showed significantly higher thermal stability as demonstrated qualitatively by a retention of colour for PGA-2. Subsequently, (re)processing was done *via* compression moulding at 250 °C for 5 min with an applied pressure of 4 tons (**Figure 3b**).

Another critical consideration when designing highly cross-linked epoxy adhesives is achieving a good balance between toughness and mechanical strength in order to avoid brittle behaviour.[6,61,62] To this end, the tensile properties of the polyamide-epoxy materials and epoxy reference were compared with respect to their apparent Young's modulus (E) and toughness (W, **Figure S8** and **Table 1**). From the stress-strain curves depicted in **Figure 3c**, an apparent shift from a brittle to a more ductile behaviour could be observed when using the dynamic polyamide curing agents. More specifically, an increase in toughness of up to a factor ~10 only came at a cost of a decrease of 10% in E with apparent values ranging from 0.3 to 0.8 GPa (measured at 20 °C). These results highlight the improved mechanical properties when introducing dynamic polyamide bonds, and in particular PGAs, into epoxy resins. However, it should be noted that the obtained results may also (partially) depend on differences in T_g between the cross-linked epoxy materials.

a) Thermal stability *b) Physical appearance*

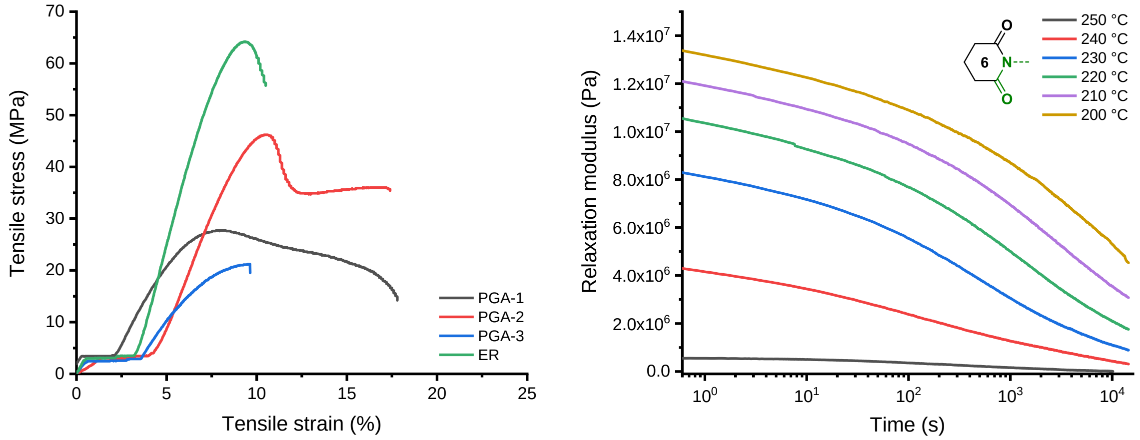

c) Tensile test *d) Stress-relaxation of PGA-2*

Figure 3. a) Photograph displaying the higher thermal stability of a PGA-cured epoxy material (PGA-2, left) compared to a previously reported dynamic polyamide network (PA ref, right) after isothermal TGA experiments at 250 °C for 2h.[57] b) Physical appearance of the reprocessed dynamic epoxy resin. c) Stress-strain curves of the dynamic epoxy materials and epoxy reference. d) Stress-relaxation data of PGA-2, highlighting the impact of bond dissociation on rheology.

Viscoelastic behaviour of dynamic polyamide-epoxy networks

Rheology measurements of the created epoxy materials were used to determine dynamic material properties. Importantly, the amount of reversible polyamide bonds was theoretically calculated to be 65-67 mol% compared to the “static” epoxy bonds (*vide supra*). As a result, sufficient activatable bonds are present to allow reprocessing into well-consolidated materials, which was verified *via* stress-relaxation experiments from 250 °C to 200 °C (**Figure S9**).[47,60] As depicted in **Figure 3d** for PGA-2, both a decrease in initial relaxation modulus (G_0 values from 1.32 10^7 to 4.2 10^6 Pa at 200 °C and 250 °C, respectively) as a result of decross-linking and an increase in relaxation (105 310 to 430 s at 200 °C and 250 °C, respectively) because of bond exchange could be observed at elevated temperatures (**Figure S10**). Moreover, relaxation followed a clear deviation from canonical single Maxwell behaviour as a result of the large structural variety of the polyamide curing agent. Therefore, calculated relaxation times (τ^*) could be obtained by a least squares fitting to a Kohlrausch-Williams-Watts (KWW) stretched exponential decay function (**eq 1**), which takes into account differences in relaxation of the composing network segments.[63–66]

$$G(t) = G_0 \, e^{(\frac{-t}{\tau})^{\beta}} \tag{1}$$

Average stretching factors (β) between 0.2 and 0.5 were obtained, which correspond quite well to values obtained for the relaxation of segmental dynamics.[67] When comparing the relaxation data in **Table 1**, a large variation could not be observed when changing the amine or ester monomer mixture, highlighting the fact that chain diffusion has a large impact on the rate of network rearrangement. This can be explained by the fact that while the rate determining step for dynamic behaviour is bond dissociation, association with another dissociated intermediate is required for bond exchange.[68] In other words, when diffusion is more difficult (e.g. in the presence of "permanent" epoxy cross-links), stress-relaxation may be slower than in a "freely moving" system. Interestingly, such diffusion is promoted when sufficient decross-linking occurs above 230 °C, resulting in the formation of free chain ends and a decrease in elasticity.

According to the Maxwell relation ($\eta[T] = G[T]\tau[T]$), both the modulus (G) related to cross-linking density and relaxation (τ) give rise to a viscosity decrease. As a result, it is worthwhile to investigate both parameters as a function of temperature (**Figure 4**).[69–71] While the rate determining step for bond exchange is the dissociation of a dicarboxamide unit (**Figure 4a**), sufficient decross-linking above 230 °C resulted in an increased relaxation rate due to the generation of free chain-ends and decrease in elasticity (**Figure 4b**). An apparent temperature dependence of material flow could then be calculated from the Maxwell relation (**Figure 4c** and **Figure S11**).

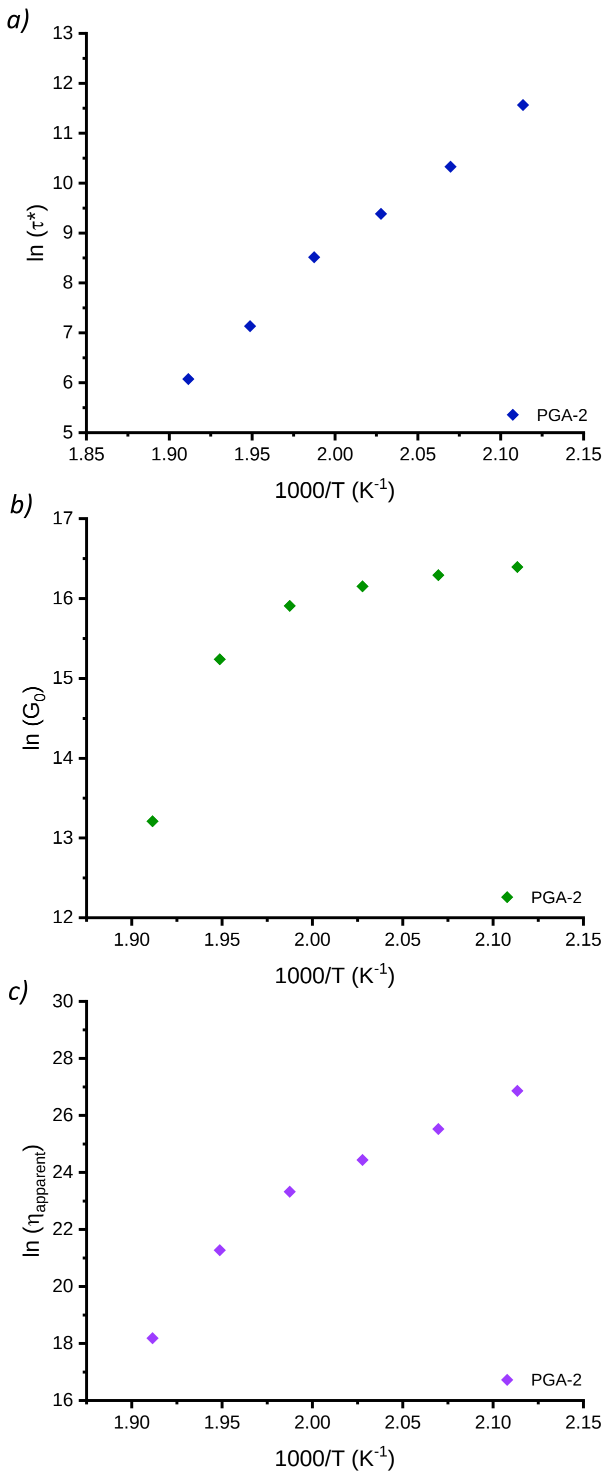

Figure 4. Temperature dependency of a) relaxation (related to Arrhenius curve), b) dissociation (related to Van 't Hoff plot) and c) apparent viscosity. It is important to note that the calculated viscosity ($\eta_{apparent}$) is similar, but not equal to the zero-shear viscosity (η_0).

By taking both relaxation and dissociation into account, an almost 3-fold increase in the slope of the viscosity curve could be determined at elevated temperatures (drop from ~10^{10} to 10^6 Pa.s). This remarkable viscoelastic behaviour demonstrates the potential of this system to show maximal viscosity during use (*i.e.* thermoset behaviour), while reaching low viscosities within the temperature range of typical nylon processing temperatures (*i.e.* 230 °C to 280 °C).[72] Importantly, the main difference between the reported system and nylon is that a viscoelastic 'melt' state is achieved through covalent decross-linking, rather than breaking inter-chain hydrogen bonds.

The decrease in modulus upon decross-linking was further characterised using frequency sweep measurements from 250 °C to 200 °C (**Figure S12**). The temperature-dependent evolution of the shear storage modulus (G') confirmed the loss of cross-linking density upon heating and recovery upon cooling. Moreover, epoxy structural adhesives are typically used at temperatures ranging from 25 to 120 °C and it is therefore critical to determine whether thermoreversibility would result in undesired debonding. To that end, creep experiments were conducted from 60 °C to 120 °C by applying a constant shear stress (σ) of 2 kPa over the course of 5000 s (**Figure S13**). The resulting strain (ε) was monitored as a function of time and an apparent creep rate ($\dot{\varepsilon}$) was obtained from the steady-state time regime.[73,74] Subsequently, zero shear viscosity (η_0) values could be determined from the Kelvin-Voigt definition ($\eta_0 = \sigma/\dot{\varepsilon}$, **Figure S14**). With the value of η_0 being between 10^{13} and 10^{14} Pa.s and only a minor decrease as a function of temperature, a high resistance to creep deformation could indeed be observed within the investigated temperature range.[75]

Adhesion properties of dynamic polyamide-epoxy networks

Following the identification of the most promising temperature range for dynamic behaviour on bulk cured samples, the potential for (de)bonding and reuse of the modified epoxy adhesives was determined using lap shear experiments (**Figure 5a**). As one of the most commonly used methods for producing data on adhesive strength, aluminium plates (length = 100 mm, width = 25.4 mm and thickness = 1.62 mm) were coated and bonded according to ASTM D 1002 by applying the adhesive mixture in a defined overlap area (15.8 mm) and subsequent curing at 120 °C for 8 h. Moreover, a wet thickness of 200 μm is targeted for each adhesive layer.

It should be noted that the absolute bonding values of commercial structural adhesives can be higher than the values reported in this manuscript due to the addition of (undisclosed) additives or cross-linkers, and such values are thus difficult to compare. However, regardless of such additives, the reference system (ER) enabled the evaluation of relative differences between reversible and irreversible adhesives. When the lap shear strength of the dynamic epoxy resins PGA-1 to PGA-3 (~ 7 MPa) was compared to the static epoxy resin ER (~ 4 MPa), a roughly 2-fold increase could be observed, as shown in **Figure 5b**. Thus, the addition of (dynamic) amide bonds increased the adhesion, which can be explained by strong (hydrogen) bonding within the bulk material and to the metal surface. Furthermore, the majority of the specimens demonstrated an adhesive type of failure (*i.e.* the adhesive separates from one of the substrates), indicating relatively strong cohesion (**Figure S15**). To initiate rebonding of the separated aluminium substrates, heating (200 °C for 2 min) and pressure (2 tons) were applied to the overlap area. The plates were then gradually cooled to room temperature to allow time/temperature for sufficient bond reconstruction. Interestingly, when the lap shear experiments were repeated on these "reused" samples, PGA-1 and PGA-2 allowed adhesive properties to be recovered up to 90 to 95 %, whereas PGA-3 only showed partial recovery up to 60 to 65 % (**Figure 5c**). As expected, the reference ER did not result in any property recovery using the same conditions.

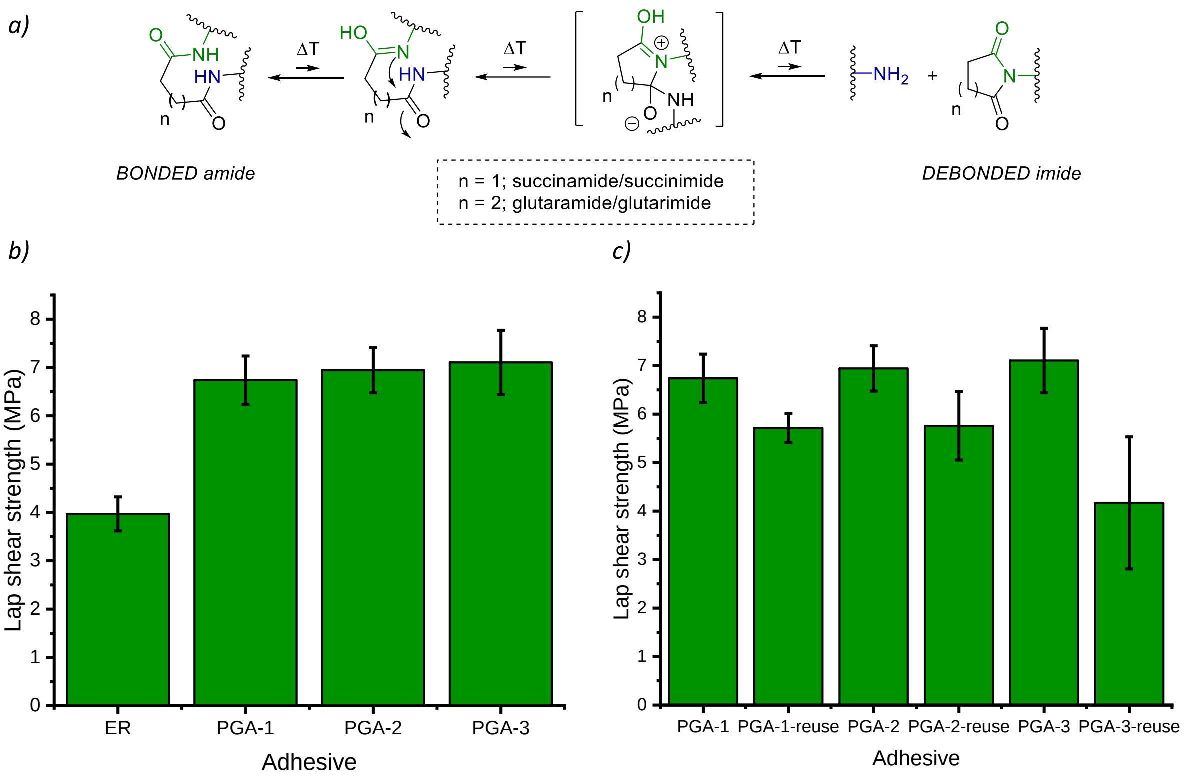

Figure 5. a) Dicarboxamide (e.g. glutaramide and/or succinamide) debonding equilibrium to a cyclic imide (e.g. glutarimide and/or succinimide) and amine. Bond strength of the dynamic epoxy resins PGA-1 to PGA-3 and reference ER measured at 20 °C a) before and b) after reusing.

The different recovery behaviour of PGA-1 and PGA-2 compared to PGA-3 could be explained by the less stable succinamide bonds (PSA hardener) compared to the glutaramide bonds (PGA hardener). As PGA-3 consists of a PGA-PSA hardener blend, it would necessitate a more regulated cooling programme. Despite this, all samples could be debonded efficiently (except ER) by exposing the bonded lap shear joints to a brief heat treatment (200 °C for 2 min) after curing and immediate cooling to room temperature. Under such cooling conditions, there is insufficient time to reconstruct bonds/interactions, which allows straightforward detachment of the substrates. From a practical standpoint, one could argue that 200 °C is a significantly high debonding temperature that may surpass the upper temperature limit of sensitive substrates. To that end, the degree of debonding of PGA-2 was determined after exposing the bonded adhesive assembly to 80 °C and 120 °C for 1 to 2 hours. **Figure S16**, shows that the bonding strength decreases as a function of temperature, which is mostly attributed to the dynamic nature of the amide bonds. However, it could be determined that at 120 °C about 30 to 35% of the bonding strength remained when compared to the bond strength at 20 °C (from ~ 7 to 2 MPa). As a result, it could be shown that the degree of debonding depends heavily on the applied temperature and exposure time and will need to be adjusted depending on the application. Moreover, to demonstrate the applicability of PGA-2 as a viable epoxy adhesive, lap shear experiments were repeated when binding stainless steel (~ 5.5 MPa) and polycarbonate (~ 3MPa) substrates and the data are included in the supporting information (**Figure S17**). As mentioned in the introduction, both cohesion and adhesion may be (independently) targeted to yield temporary adhesives.[7] For example, if dynamic bonds can be reliably broken at a small interfacial layer between the metal surface and the bulk adhesive, the entire structure should debond. However, this would necessitate the chemical attachment of a complementary reaction partner to the surface first. In industry, adhesion promoters, coupling agents, or primers are commonly used to form such an interfacial layer and to provide covalent linkages across the adhesive-adherend interface.[76] When compared to non-covalent interactions, this type of surface modification not only improves adhesion but also provides better resistance to moisture and heat. Silane primers are quite popular for surface modifications, particularly when combined with epoxy adhesives and coatings.[77–79] In the case of epoxy adhesives, complementary functional groups are typically installed via the organosilane substituent Si-R such as primary amines and epoxides, which can then participate in the curing reaction (**Figure 6a**).

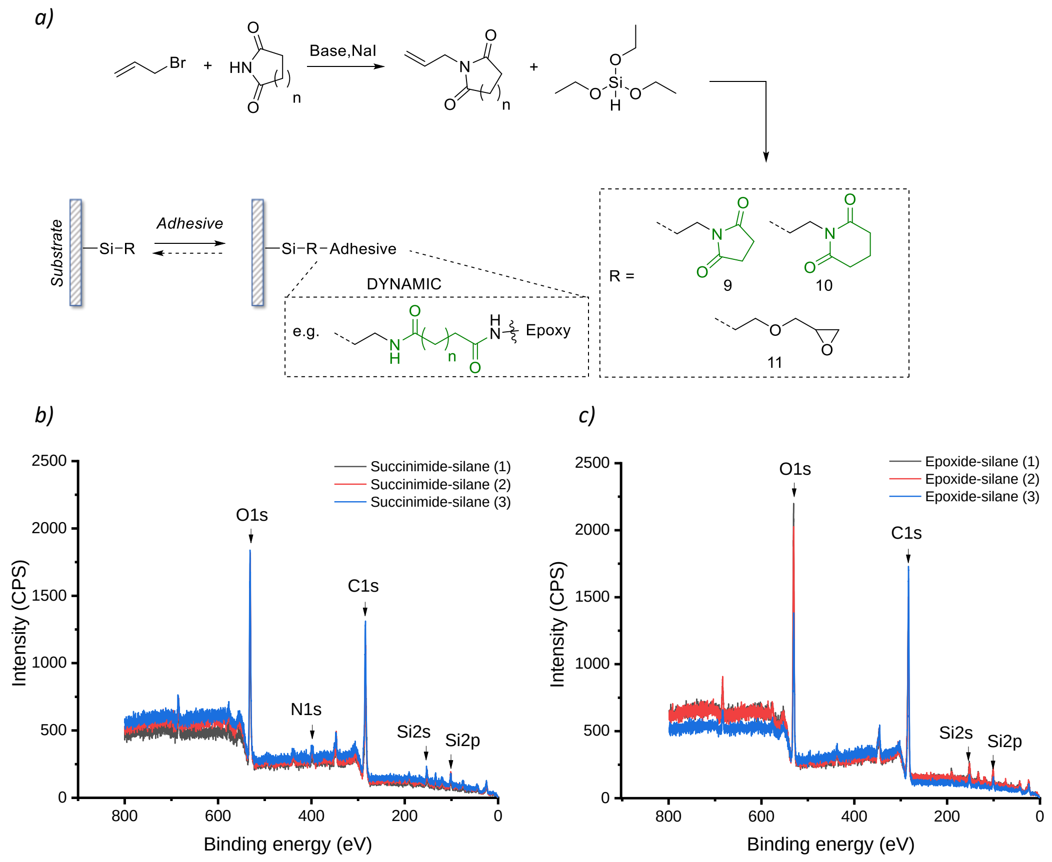

Figure 6. a) Schematic representation of a surface functionalisation with various silane primers. During adhesive curing, the complementary organic substituent (R) allows (reversible) attachment. X-ray photoelectron spectroscopy measurements with survey spectra of b) a succinimide and c) an epoxide functionalised aluminium surface.

Interestingly, by synthesising various cyclic imide-silane primers (**9**,**10**) a functionalised surface that is reactive to ring-opening with primary amines (similar to epoxide **11**) but remains dynamic is created. To that end, a two-step synthesis protocol was followed to avoid preliminary hydrolysis of the silane agent (see experimental procedures in SI and **Figure 6a**). First, an alkene-modified imide was prepared from an S_N2 reaction between succinimide or glutarimide and allyl bromide. Following that, N-allyl succinimide and N-allyl glutarimide were hydrosilylated with triethoxysilane to form the succinimide-containing compound **9** and the glutarimide-containing compound **10**.

Next, aluminium substrates were functionalised with 2 wt% of silane primer compounds **11** (a commercially available non-dynamic reference), **9** and **10** (dynamic samples) to yield surfaces that are reactive to primary amines. Application of such primers is typically done by dipping the substrate in a 4:1 ethanol:water mixture containing a specific percentage of silane coupling agent, resulting in thin coatings of 10-100 nm. Successful deposition of each primer was further verified *via* X-ray photoelectron spectroscopy (XPS, **Figure S18**). Survey scans of the surface depicted in **Figure 6b** unambiguously confirm the presence of nitrogen on the surface for the dynamic primers, which could not be detected in the case of the epoxide primer (**Figure 6c**). Furthermore, based on the intensity of the measurement, preliminary evidence is provided that only a thin polymer coating was formed (nm scale). Repeating the scan at various locations on the metal surface produced the same results, confirming complete coverage. Atomic force microscopy (AFM) was used in addition to XPS measurements to determine the modified topology and the thickness of the polymer coating deposited on each aluminium surface (20-40 nm). As shown in **Figure S19**, a clear change in surface morphology could be detected when using the silane primers, which had an important effect on the roughness.

Having successfully modified the aluminium substrates, the next step was to apply an adhesive curing formulation and demonstrate that the assembled plates could be debonded efficiently. Here it was critical to ensure that the loss in bond strength was due to a loss in adhesion rather than a change in sample cohesion. To that end, the thermoset epoxy reference ER curing formulation was used because it did not show thermal debonding from an (unfunctionalised) aluminum surface. Using the same curing conditions as mentioned in the previous section, lap shear samples ER-E, ER-S, and ER-G were obtained when silane primers **9**, **10**, and **11** were used, respectively. As shown in **Figure 7a**, all silane-modified surfaces showed an almost 2-fold increase in interfacial bond strength from 4 MPa to 7 MPa. Moreover, both surface (adhesive) and bulk (cohesive) failure could now be detected, pointing to improved attachment.

Interestingly, rebonding experiments (*i.e.* heating to 200 °C for 2 min and gradual cooling) indicated large differences in recovery of the bond strength (**Figure 7b**). As expected, the epoxide functionalised surface did not mediate any return of adhesion (see ER-E-reuse). On the other hand, the thin dynamic silane layers allowed rewetting of the metal surface and recovery up to 90 to 95 % as a result of chain relaxation in the rubber state, topological defects at the surface, and stress-relaxation when shifting the amide-imide equilibrium.[80] In addition, when studying the ruptured surface in greater detail, ATR-FTIR analysis only revealed the presence of carbonyl stretches corresponding to an amide bond for ER-S and ER-G (see **Figure 7c** around 1645 $\mathrm{cm^{-1}}$). This spectroscopic proof, combined with the relative increase in bond strength, confirmed that the imide groups of the synthesised silane primers did participate in the curing process, even when (more reactive) epoxides were present. Again, all samples could be debonded efficiently (except ER-E) by exposing the bonded lap shear joints to a brief heat treatment (200 °C for 2 min) after curing and immediate cooling to room temperature (quenched *via* liquid nitrogen). This can be understood by the fact that each substrate surface was covered with silane polymer, which significantly lost connectivity to the adhesive during dicarboxamide dissociation.

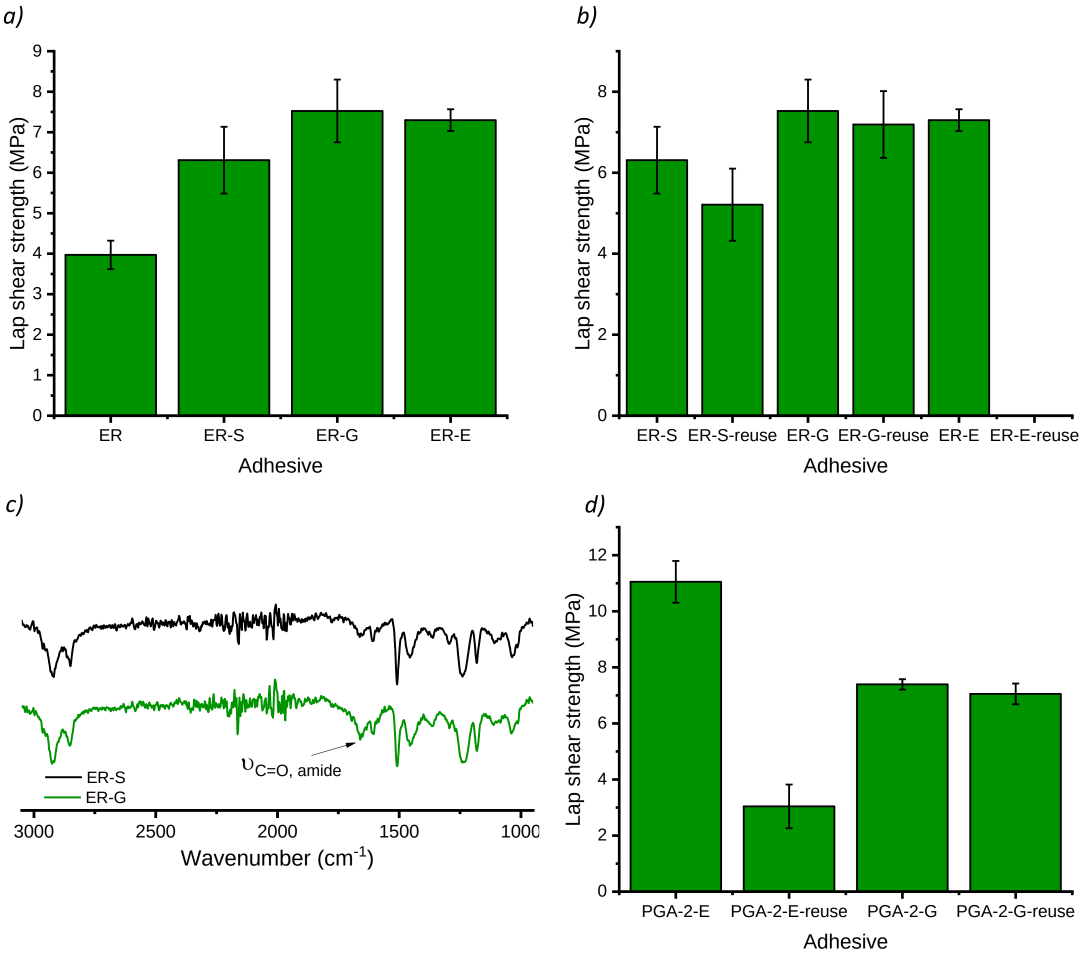

Figure 7. Bond strength of the functionalised aluminium substrates (succinimide, glutarimide and epoxide) cured with epoxy reference ER a) before and b) after reusing. c) FT-IR spectrum of the ruptured adhesive assembly modified with succinimide (ER-S) and glutarimide (ER-G) primers. d) Bond strength of functionalised aluminium substrates (glutarimide) cured with dynamic epoxy PGA-2 before and after reusing.

Motivated by their promising (de)bonding capacity, a final point of interest was to find out what would happen if the aforementioned temporary cohesion and adhesion strategies were combined into one single adhesive assembly. In that case, reversible dicarboxamide bonds would be present both in the bulk and at the adhesive interface, possibly facilitating (de)bonding and rebonding.

Indeed, when combining, for instance, the formulation corresponding to PGA-2 with 2 wt% of an epoxide-silane **11** (PGA-2-E) and glutarimide-silane **10** (PGA-2-G) functionalised aluminium surface, a drastically different behaviour in lap shear strength could be observed (**Figure 7d**).

The highest bond strength was found in PGA-2-E (~ 11 MPa), which is attributed to the difference in reactivity between the epoxide and imide functional groups. This difference in ring-opening susceptibility was accentuated by the intrinsically higher viscosity of the PGA curing agents. However, adhesion properties could only be recovered up to 30% as a result of the irreversible covalently bound silane layer that prevented reattachment. While showing a lower increase in bond strength (~ 7.8 MPa), the use of PGA-2-G resulted in up to 95% rebonding (with a low error) since both covalent adhesion and cohesion could be simultaneously restored. The origin of the differences in bond strength recovery between PGA-2-E and PGA-2-G also had a direct effect on their debonding capacity. More specifically, PGA-2-G allowed efficient debonding after heating at 200 °C for 2 min and rapid cooling, while PGA-2-E was still partially bound. Thus, interactions at the interface play an important, but often overlooked role in the overall adhesion of the system.

CONCLUSION

In summary, we have introduced a robust and easily applicable dynamic curing platform for epoxy resins, and showed its use in the design of resistant yet dynamic temporary adhesives with controlled debonding. By mixing solely commercially available monomers that are well-known to industrial formulators, PGA prepolymers were prepared that served as dynamic curing agents for epoxy materials. In comparison to an amine-hardened epoxy reference, superior thermal and mechanical properties were obtained. Furthermore, rheology experiments confirmed that when heated, a shift in the dicarboxamide-imide equilibrium allowed for the introduction of material flow only in the typical processing temperature range (230 °C to 280 °C) of thermoplastics. By applying the modified epoxy resin as an adhesive, bonding to a metal substrate increased, while debonding and rebonding properties could be introduced through reversible cohesion. On top of this, imide-silane primers were developed that allowed to independently target reversible adhesion. Using these small interfacial layers, it was shown that even without dynamic bonds in the bulk of the material, interesting thermal (de)bonding properties could be obtained. Since this surface treatment involves a simple modification of virtually any hydroxy-containing surface, it is hence believed to constitute an important addition to the realm of existing debonding technologies. Consequently, these findings will not only aid in the development of novel and industrially relevant epoxy resins, but will also provide new insights into the (de)bonding mechanism of structural adhesives.

ASSOCIATED CONTENT

Supporting Information. Containing IR spectra, DSC and TGA thermograms, stress relaxation data, frequency sweep and creep measurements of reprocessed materials, AFM measurements and XPS survey scans.

AUTHOR INFORMATION

Corresponding Author

* Filip E. Du Prez: filip.duprez@ugent.be

* Johan M. Winne: Johan.winne@ugent.be

Author Contributions

The manuscript was written through contributions of all authors. All authors have given approval to the final version of the manuscript.

Notes

The authors declare no competing financial interest.

ACKNOWLEDGMENT

F.D.P. and J.W. thank BOF-UGent for GOA-funding. F. D. P. thanks the European Research Council (ERC) under the European Union's Horizon 2020 research and innovation program (CiMaC project - grant agreement No 101021081). F.V.L. acknowledges the Research Foundation-Flanders (FWO) for his Ph.D. (Application 1S49122N) fellowship. We would like to thank Bernhard De Meyer and Jan Goeman for technical support and Dr. Nezha Badi, Dr. Kevin De Bruycker, Dr. Katrien Heyde, Dr. Bart Hommez and Tim Maiheu for fruitful discussions. We would also like to thank Lobke De Vos for XPS measurements and Seppe Van Dyck for AFM experiments.

REFERENCES

[1] A. Hutchinson, Y. Liu, Y. Lu, *J Adhes.* **2016**, *93*, 737–755.

[2] W. Li, Q. Liu, Y. Zhang, an Li, Z. He, W. C. H Choy, P. J. Low, P. Sonar, A. Ko Ko Kyaw, W. Li, et al., *Adv. Mater.* **2020**, *32*, 2001591.

[3] Y. Khan, A. E. Ostfeld, C. M. Lochner, A. Pierre, A. C. Arias, Y. Khan, A. E. Ostfeld, C. M. Lochner, A. Pierre, A. C. Arias, *Adv. Mater.* **2016**, *28*, 4373–4395.

[4] S. Leijonmarck, *Heat-Debonding Adhesives*, **2013**, US20140287299A1.

[5] J. L. Elwell, *Solvent Mixture for Dissolving and Removing Epoxy Resinous Compounds*, **1980**, US4278557A.

[6] S. Abbott, *Sticking Together: The Science of Adhesion*, Royal Society Of Chemistry, **2020**.

[7] N. D. Blelloch, H. J. Yarbrough, K. A. Mirica, *Chem. Sci.* **2021**, *12*, 15183–15205.

[8] Z. Zhang, D. Lei, C. Zhang, Z. Wang, Y. Jin, W. Zhang, X. Liu, J. Z. Sun Zhang, D. Lei, C. Zhang, et al., *Adv. Mater.* **2022**, 2208619.

[9] D. K. Hohl, C. Weder, *Adv. Opt. Mater.* **2019**, *7*, 1900230.

[10] W. Zou, J. Dong, Y. Luo, Q. Zhao, T. Xie, *Adv. Mater.* **2017**, *29*, 1606100.

[11] M. Podgórski, B. D. Fairbanks, B. E. Kirkpatrick, M. McBride, A. Martinez, A. Dobson, N. J. Bongiardina, C. N. Bowman, *Adv. Mater.* **2020**, *32*, 1906876.

[12] F. Van Lijsebetten, J. O. Holloway, J. M. Winne, F. E. Du Prez, *Chem. Soc. Rev.* **2020**, *49*, 8425–8438.

[13] F. Van Lijsebetten, T. Debsharma, J. M. Winne, F. E. Du Prez, *Angew. Chemie Int. Ed.* **2022**, *61*, DOI 10.1002/anie.202210405.

[14] H. Y. Tsai, Y. Nakamura, T. Fujita, M. Naito, *Mater. Adv.* **2020**, *1*, 3182–3188.

[15] L. Li, X. Chen, J. M. Torkelson, *ACS Appl. Polym. Mater.* **2020**, *2*, 4658–4665.

[16] B. T. Michal, E. J. Spencer, S. J. Rowan, *ACS Appl. Mater. Interfaces* **2016**, *8*, 11041–11049.

[17] E. Cudjoe, K. M. Herbert, S. J. Rowan, *ACS Appl. Mater. Interfaces* **2018**, *10*, 30723–30731.

[18] L. M. Sridhar, M. O. Oster, D. E. Herr, J. B. D. Gregg, J. A. Wilson, A. T. Slark, *Green Chem.* **2020**, *22*, 8669–8679.

[19] D. H. Turkenburg, H. van Bracht, B. Funke, M. Schmider, D. Janke, H. R. Fischer, *J. Appl. Polym. Sci.* **2017**, *134*, 44972.

[20] J. H. Aubert, *J. Adhes.* **2010**, *79*, 609–616.

[21] Wang Xiangjun, Xinzhong Li, Qi Lin, Jianrong Xia, Hanyu Xue, *RSC Adv.* **2021**, *11*, 32565–32572.

[22] A. M. Schenzel, N. Moszner, C. Barner-Kowollik, *Polym. Chem.* **2017**, *8*, 414–420.

[23] E. Trovatti, T. M. Lacerda, A. J. F. Carvalho, A. Gandini, *Adv. Mater.* **2015**, *27*, 2242–2245.

[24] S. Zhang, T. Liu, C. Hao, L. Wang, J. Han, H. Liu, J. Zhang, *Green Chem.* **2018**, *20*, 2995–3000.

[25] M. A. Rahman, C. Bowland, S. Ge, S. R. Acharya, S. Kim, V. R. Cooper, X. C. Chen, S. Irle, A. P. Sokolov, A. Savara, et al., *Sci. Adv.* **2021**, *7*, DOI 10.1126/sciadv.abk2451.

[26] Z. Zhao, P. Zhao, Y. Zhao, J. Zuo, C. Li, *Adv. Funct. Mater.* **2022**, 2201959.

[27] J.-C. Lai, J.-F. Mei, X.-Y. Jia, C.-H. Li, X.-Z. You, Z. Bao, J.-C. Lai, J.-F. Mei, X.-Y. Jia, C.-H. X. Li, et al., *Adv. Mater.* **2016**, *28*, 8277–8282.

[28] K. M. Lindenmeyer, R. D. Johnson, K. M. Miller, *Polym. Chem.* **2020**, *11*, 5321–5326.

[29] X. Chen, M. A. Dam, K. Ono, A. Mal, H. Shen, S. R. Nutt, K. Sheran, F. Wudl, *Science* **2002**, *295*, 1698–1702.

[30] B. J. Adzima, H. A. Aguirre, C. J. Kloxin, T. F. Scott, C. N. Bowman, *Macromolecules* **2008**, *41*, 9112–9117.

[31] Y. Zhang, A. A. Broekhuis, F. Picchioni, *Macromolecules* **2009**, *42*, 1906–1912.

[32] P. Du, M. Wu, X. Liu, Z. Zheng, X. Wang, T. Joncheray, Y. Zhang, *J. Appl. Polym. Sci.* **2014**, *131*, DOI 10.1002/app.40234.

[33] N. K. Guimard, J. Ho, J. Brandt, C. Y. Lin, M. Namazian, J. O. Mueller, K. K. Oehlenschlaeger, S. Hilf, A. Lederer, F. G. Schmidt, et al., *Chem. Sci.* **2013**, *4*, 2752.

[34] A. Gandini, *Prog. Polym. Sci.* **2013**, *38*, 1–29.

[35] R. C. Boutelle, B. H. Northrop, *J. Org. Chem.* **2011**, *76*, 7994–8002.

[36] X. Kuang, G. Liu, X. Dong, X. Liu, J. Xu, D. Wang, *J. Polym. Sci. Part A Polym. Chem.* **2015**, *53*, 2094–2103.

[37] F. Van Lijsebetten, K. De Bruycker, J. M. Winne, F. E. Du Prez, *ACS Macro Lett.* **2022**, *11*, 919–924.

[38] F. De Buyl, *Int. J. Adhes. Adhes.* **2001**, *21*, 411–422.

[39] S. R. Hartshorn, *Structural Adhesives: Chemistry and Technology*, Plenum Press, New York, **1986**.

[40] D. A. Dillard, *Advances in Structural Adhesive Bonding*, Elsevier, **2010**.

[41] M. M. Rahman, H.-D. Kim, W.-K. Lee, *Fibers Polym.* **2009**, *10*, 6–13.

[42] A. Murakami, D. Saunders, K. Ooishi, T. Yoshiki, M. Saitoo, O. Watanabe, M. Takezawa, *J. Adhes.* **1992**, *39*, 227–242.

[43] H.-S. Do, Y.-J. Park, H.-J. Kim, *J. Adhes. Sci. Technol.* **2006**, *20*, 1529–1545.

[44] S. Ebnesajjad, A. H. Landrock, *Adhes. Technol. Handb.* **2015**, 84–159.

[45] S. J. Monte, Springer, Dordrecht, **1998**, pp. 211–216.

[46] W. R. Ashcroft, *Chem. Technol. Epoxy Resins* **1993**, 37–71.

[47] Y. Spiesschaert, M. Guerre, I. De Baere, W. Van Paepegem, J. M. Winne, F. E. Du Prez, *Macromolecules* **2020**, *53*, 2485–2495.

[48] A. Ruiz de Luzuriaga, R. Martin, N. Markaide, A. Rekondo, G. Cabañero, J. Rodríguez, I. Odriozola, *Mater. Horizons* **2016**, *3*, 241–247.

[49] Y. Yang, Y. Xu, Y. Ji, Y. Wei, *Prog. Mater. Sci.* **2021**, *120*, 100710.

[50] Y. Sun, M. Wang, Z. Wang, Y. Mao, L. Jin, K. Zhang, Y. Xia, H. Gao, *Macromolecules* **2022**, *55*, 523–534.

[51] Q.-A. Poutrel, J. J. Blaker, C. Soutis, F. Tournilhac, M. Gresil, *Polym. Chem.* **2020**, *11*, 5327–5338.

[52] F. Van Lijsebetten, S. Engelen, E. Bauters, W. Van Vooren, M. M. J. Smulders, F. E. Du Prez, *Eur. Polym. J.* **2022**, *176*, 111426.

[53] D. Peerman, W. Tolberg, D. Floyd, *Ind. Eng. Chem.* **1957**, *49*, 1091–1094.

[54] K. Huang, J. Xia, X. Yang, M. Li, H. Ding, *Polym. J.* **2010**, *42*, 51–57.

[55] P. Vijayalakshmi, T. C. Rao, V. Kale, R. S. Balakrishna, R. Subbarao, *Polymer (Guildf).* **1992**, *33*, 3252–3256.

[56] M. Pramanik, M. Early, S. Wand, D. Gottschalk, S. K. Mendon, J. W. Rawlins, *Polym. Eng. Sci.* **2019**, *59*, E69–E81.

[57] F. Van Lijsebetten, Y. Spiesschaert, J. M. Winne, F. E. Du Prez, *J. Am. Chem. Soc.* **2021**, *143*, 15834–15844.

[58] Y. Chen, H. Zhang, S. Majumdar, R. A. T. M. Van Benthem, J. P. A. Heuts, R. P. Sijbesma, *Macromolecules* **2021**, *54*, 9703–9711.

[59] E. W. Starner, A. D. Dubowik, *Auf Gemischen von Fett- Und Aromatischen Säuren Basierende Polyamidoaminhärter*, **2000**, EP1024159B1.

[60] L. Li, X. Chen, K. Jin, J. M. Torkelson, *Macromolecules* **2018**, *51*, 5537–5546.

[61] A. J. Kinloch, *MRS Bull. 2003 286* **2011**, *28*, 445–448.

[62] S. Mostovoy, E. J. Ripling, *J. Appl. Polym. Sci.* **1971**, *15*, 661–673.

[63] M. A. Bin Rusayyis, J. M. Torkelson, *Polym. Chem.* **2021**, *12*, 2760–2771.

[64] L. E. Porath, C. M. Evans, *Macromolecules* **2021**, *54*, 4782–4791.

[65] J. L. Self, N. D. Dolinski, M. S. Zayas, J. Read de Alaniz, C. M. Bates, *ACS Macro Lett.*

2018, *7*, 817–821.

[66] J. S. A. Ishibashi, I. C. Pierce, A. B. Chang, A. Zografos, B. M. El-Zaatari, Y. Fang, S. J. Weigand, F. S. Bates, J. A. Kalow, *Macromolecules* **2021**, *54*, 3972–3986.

[67] J. C. Hooker, J. M. Torkelson, *Macromolecules* **1995**, *28*, 7683–7692.

[68] B. J. Gold, C. H. Hövelmann, N. Lühmann, N. K. Székely, W. Pyckhout-Hintzen, A. Wischnewski, D. Richter, *ACS Macro Lett.* **2017**, *6*, 73–77.

[69] C. J. Kloxin, C. N. Bowman, *Chem. Soc. Rev.* **2013**, *42*, 7161–7173.

[70] A. Jourdain, R. Asbai, O. Anaya, M. M. Chehimi, E. Drockenmuller, D. Montarnal, *Macromolecules* **2020**, *53*, 1884–1900.

[71] F. Van Lijsebetten, K. De Bruycker, E. Van Ruymbeke, J. M. Winne, F. E. Du Prez, *Chem. Sci.* **2022**, *13*, 12865–12875.

[72] R. J. Palmer, in *Kirk-Othmer Encycl. Chem. Technol.*, John Wiley & Sons, Inc., Hoboken, NJ, USA, **2000**.

[73] F. Van Lijsebetten, K. De Bruycker, Y. Spiesschaert, J. M. Winne, F. E. Du Prez, *Angew. Chemie Int. Ed.* **2022**, *61*, DOI 10.1002/anie.202113872.

[74] H. Münstedt, *J. Rheol. (N. Y. N. Y).* **2014**, *58*, 565–587.

[75] M. Capelot, M. M. Unterlass, F. Tournilhac, L. Leibler, *ACS Macro Lett.* **2012**, *1*, 789–792.

[76] P. G. Pape, *Handb. Adhes. Surf. Prep.* **2011**, 369–386.

[77] M. R. Tchoquessi Diodjo, L. Belec, E. Aragon, Y. Joliff, L. Lanarde, F. X. Perrin, *ACS Appl. Mater. Interfaces* **2013**, *5*, 6751–6761.

[78] A. Zhou, Z. Yu, H. Wei, L. H. Tam, T. Liu, D. Zou, *ACS Appl. Mater. Interfaces* **2020**, *12*, 44163–44171.

[79] T. Lin, Y. Wu, E. Santos, X. Chen, J. Kelleher-Ferguson, C. Tucker, D. Ahn, C. Mohler, Z. Chen, *Langmuir* **2022**, *38*, 2590–2600.

[80] C. Liu, D. Wang, *Macromolecules* **2022**, *55*, 1260–1266.